Review Article

NANOTECHNOLOGY BASED APPROACHES TO ENHANCE THERAPEUTIC EFFICACY OF CHLOROQUINE AND HYDROXYCHLOROQUINE – A REVIEW

ABSTRACT

Background: Chloroquine (CQ) and hydroxychloroquine (HCQ) are widely used in the treatment of endemic diseases such as malaria and autoimmune conditions like rheumatoid arthritis. Their anti-apoptotic activity, cost-effectiveness, and convenient oral administration make them effective treatments, either as standalone therapies or in combination with other drugs. However, their use is limited by a narrow therapeutic window, which can lead to potential complications due to organ accumulation and non-specific actions in healthy cells. This risk necessitates exploration into safer clinical applications using nanotechnology.**Aim:**This scoping review aims to comprehensively assess and analyze the application of nanotechnology to enhance the therapeutic efficacy and safety of CQ and HCQ.**Methods:**A meticulous search for original studies on nanoparticle formulations of “chloroquine” and “hydroxychloroquine” was conducted. Two reviewers screened titles and abstracts, followed by a detailed assessment of the full articles. Inclusion criteria encompassed original studies in English, Spanish, or Portuguese, focusing on in vitro, in vivo, and ex vivo evaluations.**Results:**After an exhaustive search across selected databases, 30 articles were meticulously chosen for comprehensive evaluation. The most common properties found for nanoparticles included sizes ranging from 100 to 300 nm, a zeta potential lower than -10, with dendritic derivatives being the most encountered types. Materials used in both production and coating varied, influencing the release and specificity of the nanocarrier. Among therapeutic activities, antimalarial and antitumor activities were the most studied.**Conclusion:**Studies have demonstrated distinct characteristics acquired by these drugs after encapsulation in various nanoparticles, including reduced toxicity, increased specificity, prolonged systemic circulation, absence of toxic peaks, and potential for different therapeutic approaches.

KEYWORDS: scope review; nanoparticulate systems; modified drug release

1. INTRODUCTION

Nanoparticles (NPs) are defined by their nanometric dimensions, ranging between 10 and 1000 nm. Their composition can vary significantly, with examples including polymers, lipids, and peptides. Regarding their structural components, certain coatings, when applied, allow for extended circulation of the nanoparticle (NP) in the bloodstream, as well as the encapsulated drug. These coatings can also act as vectors, enhancing the specificity of the therapeutic effect; an example is polyethylene glycol (PEG) (Mohanraj & Chen, 2006).

Nanotechnology, when applied to drug treatment, aims for greater efficacy and safety. It addresses various challenges, including the diffusion of insoluble drugs, maintaining the stability of unstable or low-bioavailability compounds, enhancing the specificity of drug action, and prolonging circulation time (LaVan et al., 2003).

In addition to improving drug delivery, some nanoparticles exhibit unique sensor properties due to their size and surface characteristics. These highly sensitive sensors can monitor the controlled release of encapsulated drugs and detect changes in the biological environment, such as variations in pH, ion concentrations, or specific biomarkers (Grasso et al., 2023; Joglekar & Trewyn, 2013; Lu et al., 2016; Ngoepe et al., 2013; Youssef et al., 2023). Leveraging these sensors opens up opportunities for personalized drug therapy, allowing for precise

adjustments based on individual patient needs. Recent studies (K. Jayamoorthy et al., 2023; M.M. Salem-Bekhit et al., 2023; Saravanan et al., 2016; Suresh et al., 2016; Suresh et al., 2018; Tomitaka et al., 2018) highlight the real-time monitoring ability of these sensor-enabled nanoparticles, significantly contributing to a more controlled therapeutic approach and providing valuable insights into complex interactions with biological systems.

Oral administration of free drugs is the most common method of pharmacotherapy; however, several factors can interfere with the proportion and speed of the event from administration to absorption and reaching its active site. For example, low solubility makes a drug more difficult to absorb; consequently, the concentration of the administered drug must be higher (Desai et al., 2011).

The pharmacodynamics of different drugs are directly related to the dosage of the drug and, therefore, to its effectiveness. With this in mind, there are drugs with highly responsive pharmacodynamics; these are defined as "small therapeutic window drugs," that is, small variations in systematic concentration can lead to significant changes in the drug's performance (Burns, 1999). These changes can induce side effects and toxicity traits; and, at the same time, these drugs can become ineffective when in concentrations that are considered safe. Therefore, one of the objectives of nanoformulations is to induce a prolonged and selective release of the drug, allowing for the administration of larger and more effective doses, in a sustained and, therefore, safer way (Abo-Zeid & Williams, 2019).

Chloroquine (CQ) and hydroxychloroquine (HCQ) are antimalarials belonging to the class of 4-aminoquinolines; both are formed by a flat aromatic ring and have a slightly basic character. The complexity of their pharmacokinetics and pharmacodynamics is the result of their high distribution capacity and long half-life; factors that classify them as drugs with a low therapeutic window. It is understood that the renal excretion capacity has a direct effect on increasing or decreasing the bioavailability of drugs in the body; however, their tendency to accumulate makes treatment risky (Schrezenmeier & Dörner, 2020).

Among the side effects caused by the free forms of these two drugs, the most recurrent are gastrointestinal disorders, such as abdominal discomfort, nausea, vomiting, and diarrhea. Myopathies and cardiac toxicities that can lead to heart rhythm mismatches are also adverse effects. Additionally, considering their tendency to accumulate, they can induce kidney or liver damage, whether due to insufficiency in these systems or caused by drug interaction. However, retinopathies are the most worrisome changes - as both drugs can damage retinal epithelial pigment through their lysosomal disruption mechanism (Schrezenmeier & Dörner, 2020).

Therefore, drug encapsulation aims to reduce the problems caused by the small therapeutic window, making it possible to increase doses and, therefore, guarantee the efficiency of the treatment while releasing the encapsulated drug in a controlled, prolonged, and specific way, thus avoiding the worrying accumulation and considerably reducing the adverse effects resulting from it (Stevens et al., 2020).

The mechanisms of action of CQ and/or HCQ involve immunological inhibition through the antigenic presentation and signaling pathway; interference with lysosomal and autophagic activity (Schrezenmeier & Dörner, 2020). These mechanisms can act against different pathologies, directly or symbiotically, favoring the effectiveness of pharmacotherapy. Among the objectives of the articles found in the literature, there were analyses of antimalarial activities (Muga et al., 2018; Urbán et al., 2011); antitumor activities (Arya et al., 2018); the improvement of thermodynamics therapies (Zhou et al., 2017); sonodynamics (Feng et al., 2019); and antiviral activities (Lima et al., 2018).

This scoping review aims to compile consistently, clearly, and objectively the numerous bibliographies that describe the formulation, application, and effectiveness of CQ and HCQ in an encapsulated way and on a nanometer scale. The effectiveness of these drugs is already widespread, in the same way that their toxicity and risks are well elucidated, and since they are widely implemented drugs, nanoformulations allow a new clinical

approach while maintaining responsive quality but with fewer adverse effects, greater safety, and fewer therapeutic impediments. Therefore, the main objective of this work is to allow future studies to have a solid base of information about NPs containing these drugs, their most varied clinical actions, the means, and modes of encapsulation of the compounds, the possibility of modulation, patterns of release, and the outcomes of the new pharmaceutical form.

2. METHODOLOGY

2.1. Strategic data search

A search strategy was implemented in April 2020 and included the descriptors “chloroquine,” “hydroxychloroquine,” “nanoparticles,” “nanocarriers,” “nanomedicine,” “nanosphere,” “nanostructure,” in association with the Boolean operators “AND” and “OR.” Filters for “research article,” “articles,” or “article” were also applied when these options were available in the databases. As for the year of publication, no limitation was imposed, given the low number of articles published more than 15 years ago.

2.2. Data selection

The selection of articles was performed by two independent reviewers. In case of disagreements, an external evaluator was consulted. Initially, the articles were selected by titles and abstracts, followed by a thorough reading of the full articles. The inclusion criteria encompassed complete and original articles that conducted in vitro, in vivo, and/or ex vivo studies of NP formulations containing CQ and/or HCQ, and that compared the test results (in vitro and/or in vivo and/or ex vivo) with the same drugs in their free form. Articles written in Portuguese, English, or Spanish were considered. Additionally, articles that did not qualify as “original articles,” book chapters, theses, master’s dissertations, monographs, and abstracts, as well as those that were duplicated among the databases, were excluded. Articles whose primary objective was to study NPs containing CQ and/or HCQ associated with other drugs or active substances were also not considered.

2.3. Elaboration strategy

For the development of the scoping review, the PICOS strategy was used (structured research in the acronym format; Population, Intervention, Control/Comparison, and Outcomes). This followed the recommendations of the PRISMA Extension for Scoping Reviews (Tricco et al., 2018), in which the population was tested in vitro, in vivo, and/or ex vivo in animals or cells; the intervention was NP formulations for exclusive release of CQ and/or HCQ; the control was CQ and/or HCQ in the free, non-encapsulated form; and the outcome was to evaluate the effectiveness of the administration of NPs containing CQ and/or HCQ.

2.4. Data extraction

Data extraction was performed using specific tables, prepared with relevant information about the population, intervention, control, and outcome (PICOS), in addition to other details pertinent to the objective and question of the scoping review, such as particle diameter, method of preparation, zeta potential, antimalarial and/or antitumor activity, encapsulation efficiency, cellular toxicity, and the type of study performed (in vivo, in vitro, and/or ex vivo).

3. RESULTS AND DISCUSSIONS

After conducting an advanced search in the selected databases, 1267 articles were initially identified. However, after all selection stages, only 30 articles were ultimately chosen for evaluation and discussion in this scoping

review. The flowchart detailing the entire study selection process can be observed in Figure 1.

Figure 1. Flowchart of the selection of articles related to the research topic.

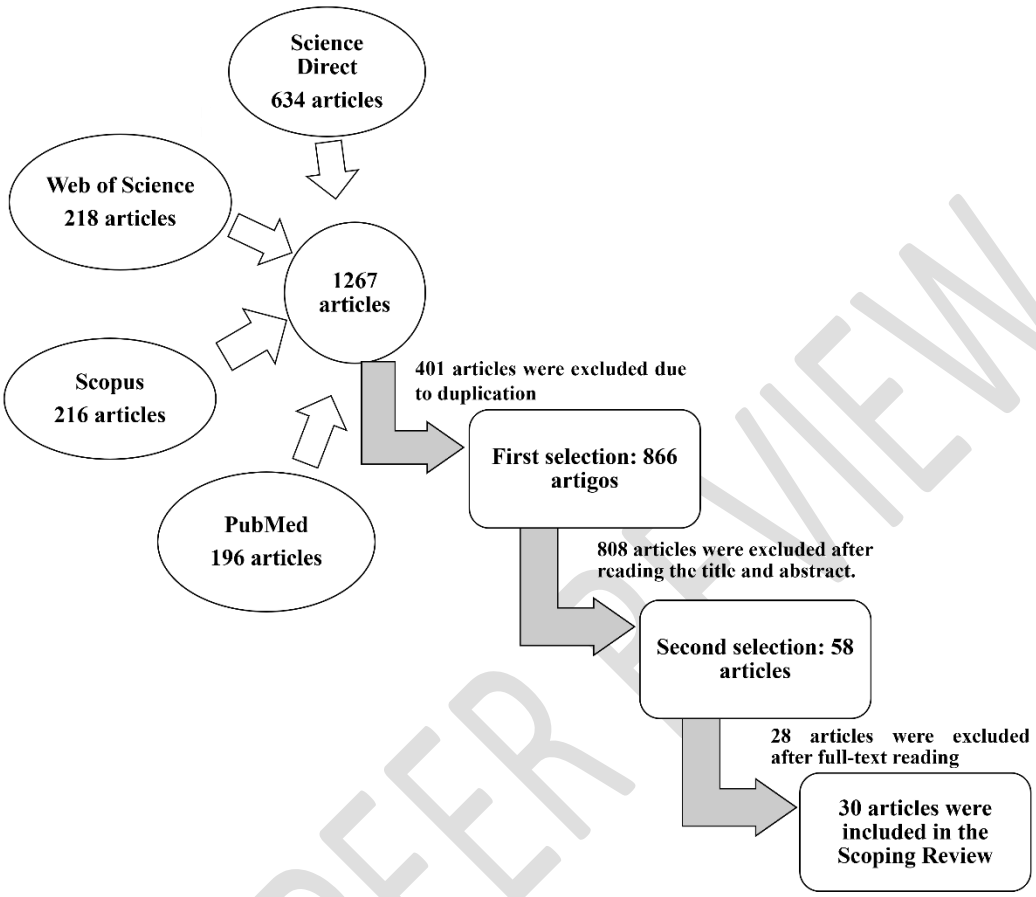

Source: The author.

3.1. Diameter of nanoparticles

According to Mohanraj and Chen (2007), the diameter of NPs and their morphology are extremely important factors in nanotechnology, as they determine the ability of biodistribution, selectivity, the level of toxicity, influence the percentage of drug encapsulated, and subsequently released. They also determine the capacity of capturing encapsulated substances by the tissues. As described in Table 1 and Figure 2, it was observed that the diameter of the NPs included in the selected articles was predominantly between 100 and 300 nm. This relatively small size is beneficial for effective cell uptake, as well as greater mobility of the drug encapsulated by the different systems of the body, and it also allows the internalization of drugs through the blood-brain barrier (Manmode et al., 2009).

Among the functional variations caused by the size of NPs, Mohanraj and Chen (2007) further speculate that the larger the particles, the larger their drug encapsulation chamber. This greater distance between the internal content of the NP and its membrane leads to a slower and more sustained release. On the other hand, the smaller the diameter of the NP, the greater its interaction with the membrane and, therefore, the faster its release into the medium. However, some factors must be considered, such as the target tissue and the caliber of the capillaries that surround it, as well as the predisposition of small-diameter NPs to aggregate.

Figure 2. Diameter of NPs

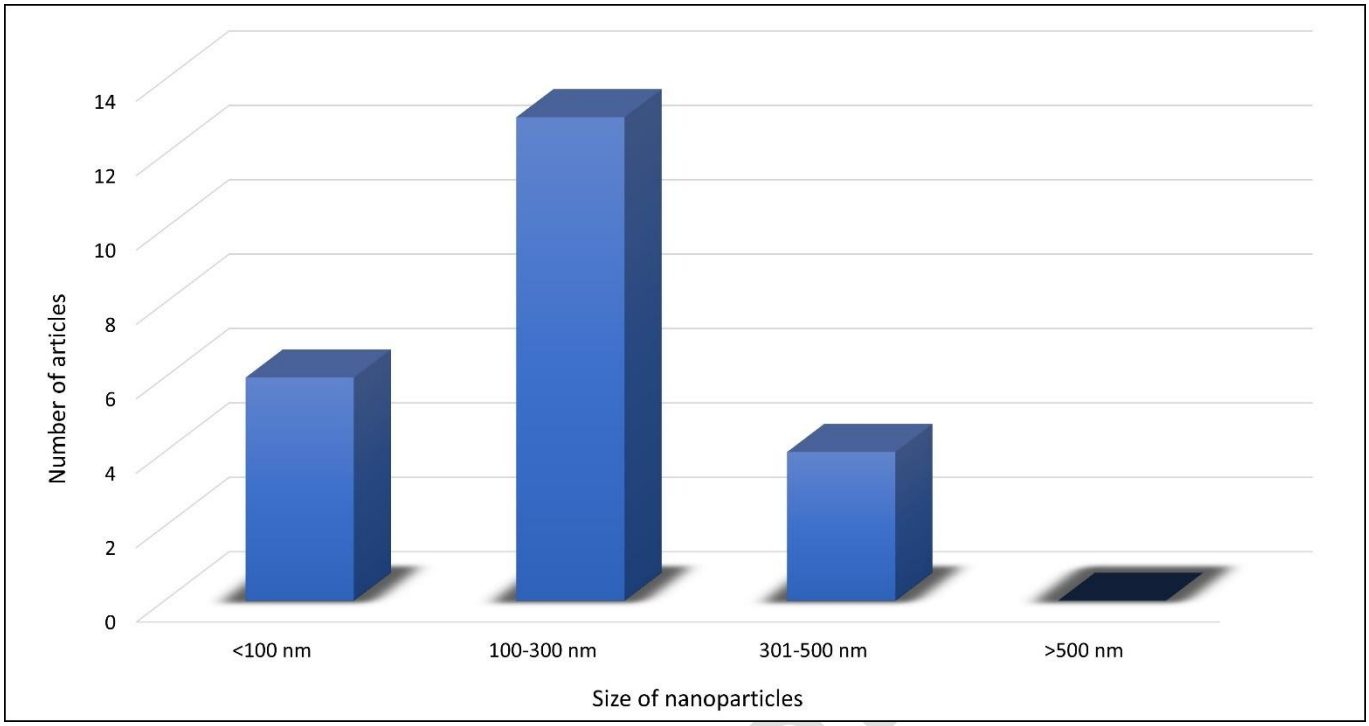

Source: the author.

Table 1- Composition, preparation, diameter, zeta potential, encapsulation efficiency and dispersion index of the NPs studied in the selected articles

References	Manuscript	Year	Type of Nanoparticles	Drug encapsulated	Composition	Coating	Synthesis method	Diameter	Zeta potential	Encapsulation Efficiency	Polydispersity Index
Movellan et al. (2014)	Biomaterials	2014	Derivatives dendritic	CQ or primaquine	Dendritic derivatives based on 2,2-bis (hydroxymethyl) propionic acid (bis-MPA) and Pluronic® polymers	NI	Emulsification oil / water	170-500nm	NI	Ranged from 81-100% as drug concentration changed	NI
Bhalekare t al. (2015)	Indian Journal of Rheumatology	2015	Solid lipid NP gel	CQ	NPs: Compritol; Gel: sodium carboxymethyl cellulose (SCMC)	NI	Sonication method with subsequent incorporation into a gel matrix	113.75 nm	NI	97.23%	NI
Zhou et al. (2017)	Biomaterials	2017	Photothermal NPs polydopamine	CQ diphosphate	Dopamine hydrochloride, Monomethoxy - polyethylene glycol with thiol end, thiol-polyethylene glycol-amine	NI	Oxidation and autopolymerization of dopamine in a mixture containing water, ethanol and ammonia with subsequent loading with CQ	120 ± 35 nm	NI	NI	NI
Chen et al. (2019)	Biomaterials	2019	Mesoporous silica NPs incorporated in bismuth	CQ	Bismuth, silica (Bi@SiO2) and poly(vinylpyrrolidone) crystals	NI	Sol-gel reaction	~250 nm	-9.6 mV.	~13.5%.	NI

Feng et al. (2019)	Acs applied materials & interfaces	2019	Mesoporous titanium dioxide NPs (hmtnps)	HCQsulfate _	Mesoporous titanium dioxide (HMTNPs)	NI	Coextrusion method after coating CCM on the surface of hmtnps /HCQ	131.7 ± 1.6 nm	-23.8 ± 0.9mV.	46.4%.	NI
Kashyap et al. (2018)	International journal of biological macromolecules	2018	Polymeric NPs	CQ	dextran (DEX)	NI	Solvent diffusion method	57.9 ± 4.6 nm	-20.1 ± 3.2 mV	81.3 ± 6.2%	NI
Ma et al. (2018)	Journal of Materials Chemistry B	2018	Mesoporous NPs	CQ	Poly(vinyl pyrrolidone) (PVP), hydrochloric acid (HCl) potassium ferricyanide and 1-tetradecanol	NI	Well-known self-conditioning method	103 ± 10.1 nm in DI water and 116 ± 6.2 nm in DMEM medium	NI	NI	NI
Liu et al. (2017)	Scientific reports	2017	Liposomes	HCQ	Cholesterol (Chl); phosphatidylcholine (PC)	NI	Film dispersion method	100-150 nm	Close to zero	NI	NI
Usmanan dAkhyar (2018)	Materials Today: Proceedings	2018	Iron polymeric NPs	CQ phosphate _	Nanoscale precursor of iron and polyethylene glycol (PEG)	NI	Formulated using the polyol method	Ni	NI	99.0%	NI

Kudirat et al. (2019)	Nanomedicine Journal	2019	Metallic NPs	CQ phosphate _	Gold, polyethylene glycol (PEG)	NI	Turkevich 's method	Range from 36.17-259.6nm based on volume of citrate used for reduction	NI	NI	NI
Bhalekar, Upadhaya andMadgulkar, (2016)	European Journal of Pharmaceutical Sciences	2016	Solid lipids NPs	CQ	Compritol , Span80 and tween 80	NI	Melt homogenization method and subjected to lyophilization	113.6 ± 0.15 nm	-27.8 ± 1.21mV	93.45 ± 0.43%	0.125 ± 0.03
Shi et al. (2018)	Biomaterials Science	2018	NPs of metallic organic structures	CQ diphosphate	Imidazolate structure zeolitic (ZIF-8)	Methoxy poly(ethylene glycol)-folate (FA-PEG)	Simple one-pot method	230 nm for CQ @ ZIF-8 and 250 nm for FA-PEG / CQ @ ZIF-8	-6.05 mV	NI	NI
Agrawal, and Jain (2007)	Biomaterials	2007	Peptides dendrimers	CQPhosphate	Poly-L-lysine; polyethylene glycol (PEG-1000) and di-tertiary butyl pyrocarbonate (di-BOC)	D-galactose	Alternation of protection and deprotection steps of L-lysine by di-BOC (di-tertiary butyl pyrocarbonate)	Uncoated 30nm; coated 50nm	NI	In uncoated NPs there was a variation of 41.4-46% and in coated NPs from 64-78%	NI
Arya et al. (2018)	Nanomedicine (london)	2018	Oxide nanoconjugate	CQ	graphite powder _	Graphene Oxide Nanosheets	Modified Hummers method	200nm	NI	77.13%	NI

Medhi et al. (2018)	Biomedical Physics and Engineering Express	2018	Mesopores	Dihydroartemisinin or CQ diphosphate	Polycaprolactone (PCL), silicon dioxide (SiO_2)	NI	Stöber's method	~450nm	−30.6 mV	NI	NI
Moles et al. (2015)	Journal of Controlled Release: official journal of the Controlled Release Society	2015	Liposomes	CQ or primaquine	Neutral charge unsaturated (DOPC: cholesterol, 80:20) or saturated (DSPC: cholesterol, 90:10) phospholipids	anti-GPA	Lipid film hydration method	NI	NI	98.3%	NI
Limaet al. (2018)	Pharmaceutics	2018	Polymeric NPs	CQ diphosphate	Poly (acid lactic) (PLA)	NI	Solvent emulsification-evaporation method	<300 nm	-20mv	64.10%	NI
Mugaet al. (2018)	Malaria journal	2018	Heparin-functionalized solid lipid NPs (Hep-slns)	CQ	Poly(polyvinyl alcohol) (PVA); stearic acid ; chitosan; d-lactose monohydrate , sulfanoyl	Heparin	Double emulsification technique with solvent evaporation	374.6 ± 7.6 nm	-4.06+- 0.091 mv	78%	0.72+- 0.053
Crommelin et al. (1991)	Journal of Controlled Release	1991	Liposomes	CQ	Lipid composition (molar ratio) was: DSPC, DPPG and chol 10: 1: 10	NI	Reverse phase evaporation method	Ni	NI	NI	NI

Fotoran et al. (2019)	Nanomedicine	2019	Multilamellar liposomes	CQ or artemisin	Lipids (1,2-Dioleoyl-*sn -glycero* -3-phosphocholine, 1,2-dipalmitoyl80 galloylglycerol , amine-N-[4-(p -malimidophenyl) butyramide)	NI	Lipids mixed in a molar ratio of 5 : 1 : 4 (Avanti Polar Lipids) and dried under N2 flow	50 nm	NI	average of 77.7%	NI
Tripathy et al. (2018)	Asian Pacific Journal of Tropical Medicine	2018	Polymeric NPs	CQ	Chitosan Tripolyphosphate (CS-TPP)	NI	Gelling method ionotropic	Ni	NI	NI	NI
Urbán et al. (2011)	Journal of Controlled Release	2011	Immunolipos omes	CQ	Lipids (phosphatidylcholine), PC; phosphatidylethanolamine , PE; cholesterol; 1,2-dioleoyl-sn-glycero-3-phosphatidylcholine, DOPC)	Semiantibodies containing a free thiol group	Lipid film hydration method	Ni	NI	NI	NI
Tripathy et al. (2013)	Acta Tropica	2013	Polymeric NPs	CQ	Chitosan and Sodium Tripolyphosphate	NI	Gelation between chitosan and sodium tripolyphosphate	Ni	NI	NI	NI

Baruah,et al. (2018)	Journal of Drug Targeting	2018	Nanostructured carriers lipids	CQ phosphate	Capmul MCM (liquid lipid) and GMS (solid lipid). [solid-liquid lipid mixture in a ratio of 80:20	NI	Microemulsification	61.7 -150 nm	+11.2 to +39mv	63.7-92.4%	NI
Bhadra, Bhadra and Jain(2006)	Pharmaceutical research	2006	Peptides dendrimers	CQ	PEG- lysine	Some were coated with Chondroitin Sulfate A (CSA)	Dialysis	10-30 nm uncoated and 100 nm coated	NI	It ranged from 3.0% to 27.5% according to the formulation	NI
Coma-Cros et al. (2018)	Pharmaceutics	2018	Dendrimers	CQ	Polyamidoamine Polycation Polymer (PAA)	NI	CQ was added dropwise to the solution containing the polymer/polymers	50-400nm	NI	NI	NI
Tripathy et al. (2014)	European Journal of Pharmacology	2014	Dendrimers	CQ	Chitosan and tripolyphosphate	NI	Gelation ionotropic	150-300 nm	+32.9 mV	NI	NI
Urbán et al. (2011)	Nanoscale Research Letters	2011	Immunolipos omes uni or bilamellar	CQ or phosmidomycin	Lipid formulation 1,2-dioleoyl- *sn* glycero-3-phosphatidylcholine [DOPC]; Cholesterol (80:20); - 1,2-dipalmitoyl-sn-glycero-3-phosphoethanolamine	BM1234 antibodies	Lipid film hydration method	Average size 200nm and a minimum threshold of 100nm	NI	NI	NI

					N- [4-(p - maleimidophenyl) butyramide]						
Stagni et al. (2020)	International Journal of Pharmaceutics	2020	Dendrimer associated/functionalized with trienylphosphonium cation	CQ	Triphenylphosphonium cation ($TPP^{+)}$ and Polyethyleneimine (PEI)	NI	Addition drop by drop	Less than 100 nm	NI	NI	NI
Joshi et al. (2012)	Colloids surf b biointerfaces	2012	Metallic gold NPs	CQ	Gold(III) ions, sodium borohydride , 11-mercaptoundecanoic acid	NI	Reduction of gold (III) ions with sodium borohydride	7 ± 1.5 nm	NI	78.7%	NI

NI = Not informed; CQ = Chloroquine; HCQ = hydroxichloroquine; NPs = Nanoparticles; NP = Nanoparticle

3.2. Types of nanoparticles

It was analyzed that each NP formulation gives a characteristic diameter to the carrier, in the same way that the target cell and/or tissue must be compatible with the choice. As can be seen in Table 1 and Figure 3, among the thirty articles selected: four were liposomes, which are spherical vesicles composed of one or more phospholipid bilayers. Their use is advantageous since they are stable carriers with a long half-life and, when coated with hydrophilic compounds or targeting molecules, they manage to escape phagocytosis (Stevens et al., 2020).

In five articles, polymeric NPs were produced, which are composed of amphiphilic polymers that precipitate with the encapsulated drugs, forming a hydrophobic cavity and a hydrophilic outer membrane. They are generally used to improve the solubility of poorly soluble drugs and facilitate their dispersion in tumors. Their low critical micellar concentration leads to even greater stability than other micellar surfactants (Stevens et al., 2020).

In another six articles, dendritic derivatives were developed, which are composed of macromolecular polymers and span several generations, favoring drug encapsulation and transport. The variability in their morphology, size, nucleus polarity, and terminal groups allows a better adaptation to the compound that is desired to be encapsulated (Stevens et al., 2020).

Four articles used solid lipid NPs, which have a lipid composition but differ from liposomes in the absence of a nucleus. These are generally implemented to increase the solubility of hydrophobic drugs in oral administration, as they have high biocompatibility and biodegradability (Stevens et al., 2020).

Metal NPs were studied in three other bibliographies. These have been implemented for the transit of drugs that have functional groups that induce their chelation with the metal of the NP, an example given by Stevens et al. (2020) was the link between compounds with a thiol group carried by gold particles, which exchanged their Au-thiol pairing for the interaction with intracellular glutathione and thus released the drug.

Only one article developed graphene oxide nanoconjugates, which impregnate other carriers, thereby favoring their endosomal/lysosomal uptake and thus making the drug's action more cytotoxic on target cells. Likewise, its conductivity enhances the pharmacological effectiveness of photothermal and photodynamic therapies (Arya et al., 2018).

Two articles described the performance and production of immunoliposomes, which are liposomes functionalized with monoclonal antibodies or antibody fragments. In addition to the innate ability of liposomes to carry and release drugs in a prolonged manner, the presence of the antibody confers greater specificity to the drug site of action, directing it to cells with overexpression of the antigen corresponding to the antibody used (Eloy et al., 2017).

Mesoporous silica NPs were evaluated in four articles, which describe that their colloidal metal oxide composition provides a porous and siliceous surface, allowing for great variability in size, morphology, and loading capacity. The presence of pores confers the greatest advantage, which is the property of adsorption and effective transport of a wide range of biomolecules and therapeutic agents, ensuring a controlled release (Manzano & Vallet-Regí, 2020).

Finally, a single article produced photothermal NPs, which can be composed of different molecules and guarantee high thermal and photodynamic resistance, thus favoring photo-dependent therapies. In the selected article, the composition was polydopamine, which is the oxidized and self-polymerized form of the dopamine molecule. The use of PDA was initially described for the surface modification of NPs, providing them with greater adhesion and enabling the formulation of nanometric films with low

toxicity and high chemical and thermal stability. However, new bibliographies confirm that the coating still confers solubility in water and isoelectricity at pH 4.5, favoring the penetration of drugs in mucous membranes at biological pH (Poinard et al., 2018).

Figure 3 - Types of nanoparticles

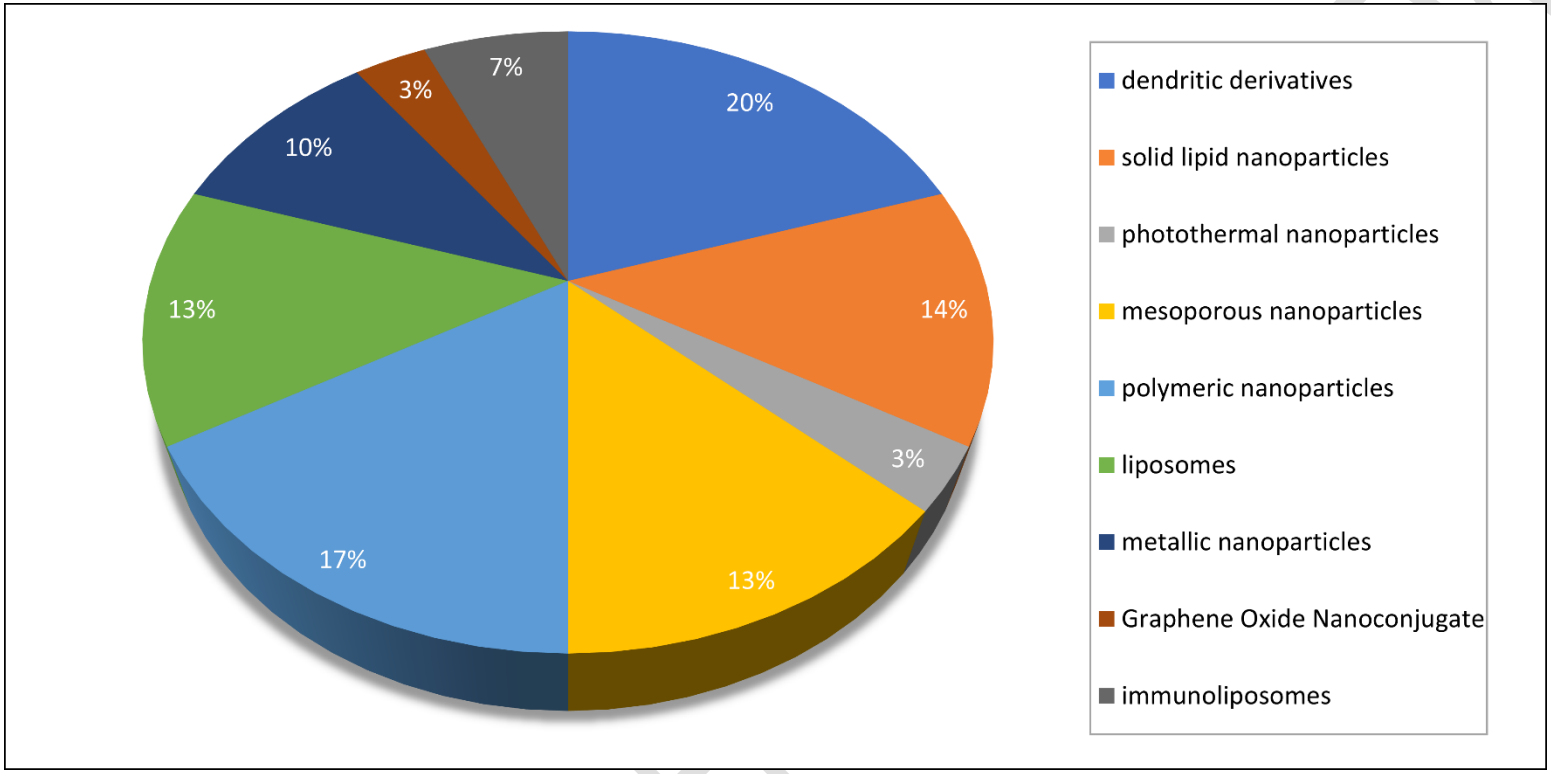

Source: the author.

3.3. Zeta potential of nanoparticles

Honary and Zahir (2013) define the zeta potential as the average electrostatic potential between the charges that surround an NP in colloidal dispersion and the charges of the liquid medium of the dispersion. They describe that this property significantly interferes with the pharmacokinetics of NPs. The charge influences the opsonization and phagocytosis capacity of NPs, allowing for modulation and targeting, and ensuring that they are effective before being degraded.

Therefore, as can be seen in Table 1 and Figure 4, in five articles, zeta potentials with values lower than -10 mV were obtained; values between -10 mV and +10 mV were found in four articles, however, only two articles obtained NPs with surface charges above +10 mV.

In another review work, Honary and Zahir (2013) addressed the effects of zeta potential on the pharmacological properties of nanocarriers. The controlled release would be modulated by the interaction of the encapsulated drug with the material that composes the nanocarrier, so the zeta potential would allow an interaction of greater or lesser scale, and this would influence the speed of drug release in the biological environment. In addition, it would also contribute to drug loading efficiency, with the carrier's surface zeta potential and the type of binding it establishes with the drug being the most relevant factors for this parameter. This said interaction would also determine if the drug would stay inside the NP or if it would be adsorbed to it.

Lowry et al. (2016) explain that values of ±30 mV are physically stable, as they prevent the aggregation of NPs through electrostatic repulsion forces. Similarly, the study by Doostmohammadi et al. (2011) reinforces that, for particles of small diameter, high values of zeta potential (negative or positive) reduce the risk of aggregation, whereas lower values have a greater tendency to aggregate.

From another perspective, Zhang et al. (2007) describe that NPs with negative zeta potential tend to be endocytosed by normal breast epithelial cells MCF10A and that this process leads to an increase in the surface charge (also negative) of these cells, reducing their values in modulus; in comparison, cancer cells like MCF7 tend to have their zeta potential reduced as they adsorb the negatively charged NPs, making them even more negative. This information indicates that the zeta potential induces a specific functionality with normal cells and cancer cells and can be implemented for characterization purposes.

Figure 4 - NPs zeta potential

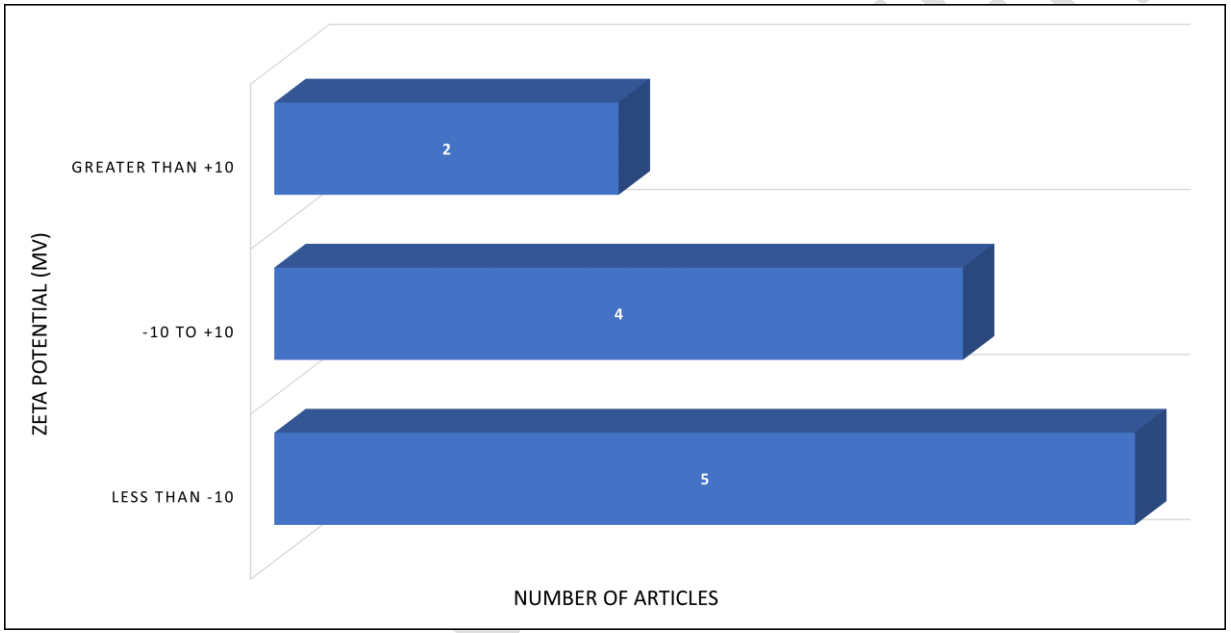

Source: the author.

3.4. Preparation of NPs

As previously mentioned, nanoformulations can take different forms, and for this to be possible, there are various methods of preparation. Ealias and Saravanakumar (2017) describe the synthesis methods based on their classification: constructive methods, where atoms are transformed into clusters and these into NPs (for example, sol-gel reaction and biosynthesis), as opposed to destructive methods, where a bulky material is degraded to a nanometer scale through milling (most common), crackling, nanolithography, and thermal decomposition.

As can be seen in Table 1, the following methods were used: sol-gel reaction (Chen et al., 2019); oil/water emulsion or solvent diffusion method (Kashyap, A., Kaur, R., Baldi, A., Jain, U. K., Chandra, R., Madan, 2018; Movellan et al., 2014); sonication method (Bhalekar et al., 2015), oxidation and auto-polymerization method (Zhou et al., 2017); co-extrusion method (Feng et al., 2019); self-conditioning method (Ma et al., 2018); film dispersion method (Liu et al., 2017); Usman polyol method (Usman and Akhyar Farrukh, 2018); Turkevich's method (Kudirat et al., 2019); homogenization and lyophilization method (Bhalekar, Upadhaya, P. G., & Madgulkar, A. R., 2016); simple one-pot method (Shi et al., 2018); alternating protection and unprotection method (Agrawal et al., 2007); modified Hummers method (Arya et al., 2018); Stober's method (Medhi et al., 2018); reverse phase evaporation method (Crommelin et al., 1991); conjugation lipid (Fotoran et al., 2019); microemulsification (Baruah et al., 2018); dropwise addition (Coma-Cros et al., 2018; Joshi et al., 2012; Stagni et al., 2020); ion reduction (Joshi et al., 2012); simple and double emulsification method with solvent evaporation (Lima et al., 2018; Muga et al., 2018); and dialysis (Bhadra, Bhadra, S., & Jain, N. K., 2006).

Among the articles, the most recurrent methods were hydration of the lipid film (Moles et al., 2015; Urbán et al., 2011b, 2011a), a process in which surfactants and cholesterol are dissolved in an organic solvent, which is then evaporated at low pressure and a buffer solution is added – the result is a hollow ''shell'' composed of a thin lipid layer (Amoabediny et al., 2018).

Also, the ionotropic gelling method (Tripathy et al., 2018, 2014, 2013), where biodegradable hydrophilic polymers such as chitosan, which have a positive surface charge, are used to interact with a negatively charged polymer and form nanometer-scale coacervates (Nikam et al., 2014).

3.5. Drug encapsulation efficiency

Analyzing Table 1, it is observed that only sixteen of the thirty articles presented the value of encapsulation efficiency, among these, eleven had an efficiency above 70% (Arya et al., 2018; Baruah et al., 2018; Bhalekar, Upadhaya, P. G., & Madgulkar, A. R., 2016; Bhalekar et al., 2015; Fotoran et al., 2019; Joshi et al., 2012; Kashyap, A., Kaur, R., Baldi, A., Jain, U. K., Chandra, R., Madan, 2018; Moles et al., 2015; Movellan et al., 2014; Muga et al., 2018; Usman and Akhyar Farrukh, 2018).

The highest encapsulation efficiency obtained was described by Usman and Akhyar Farrukh (2018), which reached 99% in the encapsulation of CQ phosphate in iron polymeric NPs. It is deduced that the interaction of polyethylene glycol, which is a highly hydrophilic polymer (Van Vlerken et al., 2007), with CQ phosphate, which is a weak base and also water-soluble (Pelt et al., 2018), would be responsible for the high capacity of the carrier to encapsulate the drug.

Regarding the five remaining articles, Chen et al. (2019) obtained the lowest encapsulation efficiency (~13.5%) when using mesoporous silica NPs incorporated in bismuth – a carrier that establishes a weak interaction with the encapsulated drug, which adsorbs in its pores and, therefore, results in low encapsulation efficiency (Kankala et al., 2019). In the second study, the work by Bhadra, Bhadra, S., & Jain, N. K. (2006) appears, obtaining 27.5% ± 3% of encapsulation efficiency with peptide

dendrimers. The other carriers obtained efficiency between 40% and 70% and were developed by Feng et al. (2019) - hollow mesoporous titanium dioxide NPs; Agrawal et al. (2007) - peptide dendrimers (the formulation encapsulated with D-lactose showed an increase in efficiency, 64 to 78%, compared to the non-encapsulated form - 41 to 46%) and finally Lima et al. (2018) who obtained 64.10% efficiency using polymeric NPs.

3.6. Composition of the nanoparticle

As can be seen in Table 1, the composition has a close relationship with the type of NP synthesized and the method chosen for this. When dendritic derivatives were synthesized, they were based on: 2,2-bis(hydroxymethyl) propionic acid (bis-MPA) and Pluronic® polymers; a combination of poly-L-lysine, polyethylene glycol (PEG-1000), and di-tertiary butyl pyrocarbonate (di-BOC); PEG-lysine; polyamidoamine (PAA) polycation polymer; chitosan and tripolyphosphate; and finally, triphenylphosphonium cation (TPP+) and polyethyleneimine (PEI). It was observed that the most recurrent composition was polyethylene glycol and lysine, which appears in two of the six articles that synthesized the dendritic derivatives (Agrawal et al., 2007; Bhadra, S., & Jain, N. K., 2006). The synthesis of dendritic micelles with polyethylene glycol and poly-L-lysine was used by Bhadra et al. (2005) in yet another of their works with the objective of developing an amphiphilic carrier that increases the solubility of insoluble drugs, also having a greater interaction and favoring encapsulation, as well as increasing generations of the dendritic derivative will reduce drug escape.

As for solid lipid NPs, the composition varied between: compritol; compritol, span 80, and tween 80 surfactant; a conjugate of poly(polyvinyl alcohol) (PVA), stearic acid, chitosan, d-lactose monohydrate, sulfanoyl; capmul MCM (liquid lipid), and GMS (solid lipid). Compritol was the most used, appearing in two of the four articles on solid lipid NPs (Bhalekar & Upadhaya, P. G., & Madgulkar, A. R., 2016; Bhalekar et al., 2015). As found by Alex et al. (2011), compritol is an extremely biocompatible, biodegradable, and non-toxic compound which, when implemented in NPs, increases the lymphatic uptake and blood circulation of the drug. Likewise, it could enter the central nervous system, becoming a carrier of high clinical value.

The only article that includes photothermal NPs in this review was composed of dopamine hydrochloride and monomethoxy-polyethylene glycol (Zhou et al., 2017). Zhu & Su (2017) describe that dopamine is an excellent photothermal agent with high infrared absorption and high photothermal energy conversion efficiency. In the same way, its conjugation with polyethylene glycol derivatives increases its circulation time in the body.

The mesoporous NPs were composed of bismuth, silica (Bi@SiO2), and poly(vinylpyrrolidone) crystals; mesoporous titanium dioxide (HMTNPs); poly(vinyl pyrrolidone) (PVP), hydrochloric acid (HCl), potassium ferricyanide, and 1-tetradecanol; and polycaprolactone (PCL) with silicon dioxide (SiO2). It is observed that the most used were poly(vinyl-pyrrolidone) and silicon dioxide (SiO2) - in two articles each (Chen et al., 2019; Ma et al., 2018; Medhi et al., 2018). Wang et al. (2019) explains that the use of silicon dioxide is common in mesoporous NPs because it acts as a highly stable adsorbent, is financially satisfactory, and provides the ability to control the diameter and distribution of pores on the surface of the carrier, thus promoting better dispersion in water.

Polymeric NPs were developed with dextran; iron and polyethylene glycol precursors; poly(lactic acid) (PLA) and chitosan-tripolyphosphate (CS-TPP), which had the highest occurrence (in two of the five articles) (Tripathy et al., 2018, 2013). In the study by Bangun et al. (2018), the properties of chitosan, such as biocompatibility, low

immunogenicity, and highly positive charge that favor adhesion to the mucosa, are well elucidated. Its interaction with tripolyphosphate, which is a crosslinking agent, fortifies and makes its degradation into smaller NPs more difficult.

The liposomes were composed of: Cholesterol (Chl) and phosphatidylcholine (PC); neutrally charged (DOPC: cholesterol, 80:20) or saturated (DSPC: cholesterol, 90:10) unsaturated phospholipids; lipid mixture of DSPC, DPPG, and chol (10:1:10); and likewise, another lipid interaction (1,2-Dioleoyl-sn-glycero-3-phosphocholine, 1,2-dipalmitoyl-80 galloyl glycerol, amine-N-[4-(p-maleimidophenyl) butyramide). It is observed that the presence of cholesterol is a common feature in three of the four articles included: Crommelin et al. (1991), Liu et al. (2017), and Moles et al. (2015). Nie et al. (2012) describes the role of cholesterol as a structuring agent of the liposomal membrane, and its charge and the presence or absence of polyethylene glycol coating are directly related to the reduction of fluidity and selective permeability of the membrane.

In the three articles that describe the synthesis of metallic nanoparticles, imidazolate zeolitic structure (ZIF-8); gold, polyethylene glycol (PEG), and a union of gold (III) ions, sodium borohydride, 11-mercaptoundecanoic acid were used. Gold-compounded NPs proved to be popular not only among the articles in this selection (Joshi et al., 2012; Kudirat et al., 2019). Its wide use can be explained by its high affinity with surface ligands, such as proteins, antibodies, and thiol functional groups, which can be implemented as a target selectivity strategy (Mody et al., 2010).

Only one graphene oxide nanoconjugate was included in this review - Arya et al. (2018) - and its composition is graphite powder. Nanomaterials made of carbon have great prominence for their unique property as an adsorbent for liquid or gaseous phases – being widely used as a removal agent for environmental pollutants (Odiogenyi, 2019).

The two remaining articles, by Urbán et al. (2011b, 2011a), describe the preparation of immunoliposomes, of lipid composition (phosphatidylcholine, PC; phosphatidylethanolamine, PE; cholesterol; 1,2-dioleoyl-sn-glycero-3-phosphatidylcholine, DOPC); Cholesterol (80:20); 1,2-dipalmitoyl-sn-glycero-3-phosphoethanolamine-N; [4-(p-maleimidophenyl) butyramide]. The recurrence of cholesterol is again observed, which can be explained by the fact that they are also liposomes, however, functionalized with monoclonal antibodies or fragments thereof (Eloy et al., 2017).

3.7. Coating

Nanocarriers began to be implemented in pharmacotherapeutics to increase drug solubility, reduce their toxicity, improve their selectivity, and increase their circulation time in the bloodstream. However, as they are foreign bodies to the organism, their presence could generate immunogenicity and induce early uptake of carriers by phagocytes. In this context, there are several studies on ways to cover up the NPs so that they go unnoticed by the immune system and thus reach their site of action (Yee Fam et al., 2020).

Among the thirty articles in this review described in Table 1, only eight presented coating. Three of them are immunoliposomes, therefore having an antibody coating or part of them. Moles et al. (2015) used anti-GPA antibodies, which act on glycoprotein A present in red cells infected or not by *P. falciparum* – the drug acts on the microorganism or performs prophylactic action (Coma-Cros et al., 2018). Urbán; Estelrich; Cortés et al. (2011) functionalized liposomes with semi-antibodies containing a

free thiol group. In another article, Urbán et al. (2011b) used the monoclonal antibody BM1234, which acts against the histidine-rich membrane protein expressed by *P. falciparum* (Marques et al., 2017).

Bhadra, S. & Jain, NK (2006) coated a part of their peptide dendrimers with chondroitin sulfate A (CSA), which is widely used because it is a glycosaminoglycan sulfate that diffuses widely in the extracellular membrane of animal tissues and manages to reach the nervous tissue, constituting a neuronal system that surrounds the sum of the neurons (Nie et al., 2019).

Muga et al. (2018) functionalized their solid lipid NPs with heparin, an anticoagulant that minimizes thrombus formation and improves carrier hemocompatibility (Luo et al., 2018).

Arya et al. (2018) made the coating with graphene oxide nanosheets, which, as already mentioned, have an excellent adsorption capacity.

Agrawal, Gupta, and Jain (2007) used D-galactose to coat their peptide dendrimers; it is understood that the presence of carbohydrates on the carrier surface induces endocytosis via lectin receptors, which are highly expressed at strategic points, such as in alveolar, peritoneal, and brain macrophages (Jain et al., 2015).

Finally, Shi et al. (2018) coated the metallic NPs with methoxy poly(ethylene glycol)-folate (FA-PEG). PEG is popularly implemented because it reduces the adsorption capacity of proteins on the surface of the NP, thus minimizing their phagocytosis. Likewise, folate receptors are used as targeting molecules, since overexpression occurs in cancer cells such as epithelial carcinoma (Yoo et al., 2012).

3.8. Polydispersity index

When NPs are synthesized in a colloidal medium, they are expected to assume similar and specific diameters, morphologies, and chemical properties, since a large-scale variation can interfere with the final objective of the formulation. In this way, the polydispersity index quantifies the level of this variation in the diameter of the NPs within the same colloidal solution, which can be altered by the formation of aggregates, adsorption of proteins on the surface of the NP (corona protein), or due to the mode of synthesis used (Johnston et al., 2018).

Some methods such as scanning/transmission electron microscopy (SEM/TEM), dynamic light scattering (DLS), and X-ray diffraction (XRD) can be used for characterizing the size of NPs and calculating the polydispersity index (Tomaszewska et al., 2013).

Among the articles in this review, only two presented the polydispersity index, Bhalekar et al. (2016) and Muga et al. (2018); which were, respectively, 0.125 ± 0.03 and 0.72 ± 0.053 (as shown in Table 1). According to Shazly (2017), indices smaller than 0.3 are considered ideal and represent a low variation in size between the NPs in the solution - values below 0.1 would be considered monodispersions; that is, the lower the polydispersity index, the greater the homogeneity of diameters and more effective the transport of compounds and thermo/luminous dispersion in phototherapies.

3.9. Cytotoxicity in Tumor Cells

Figure 5 presents the different properties of NPs containing CQ and/or HCQ in the thirty articles included in the selection. Table 2 discusses the eight articles that explored the implementation of these drugs in the treatment of tumors, while Table 3 focuses on the antimalarial effect, which was the most frequently studied aspect, observed in thirteen different articles.

Figure 5 - Therapeutic activities of the NPs tested

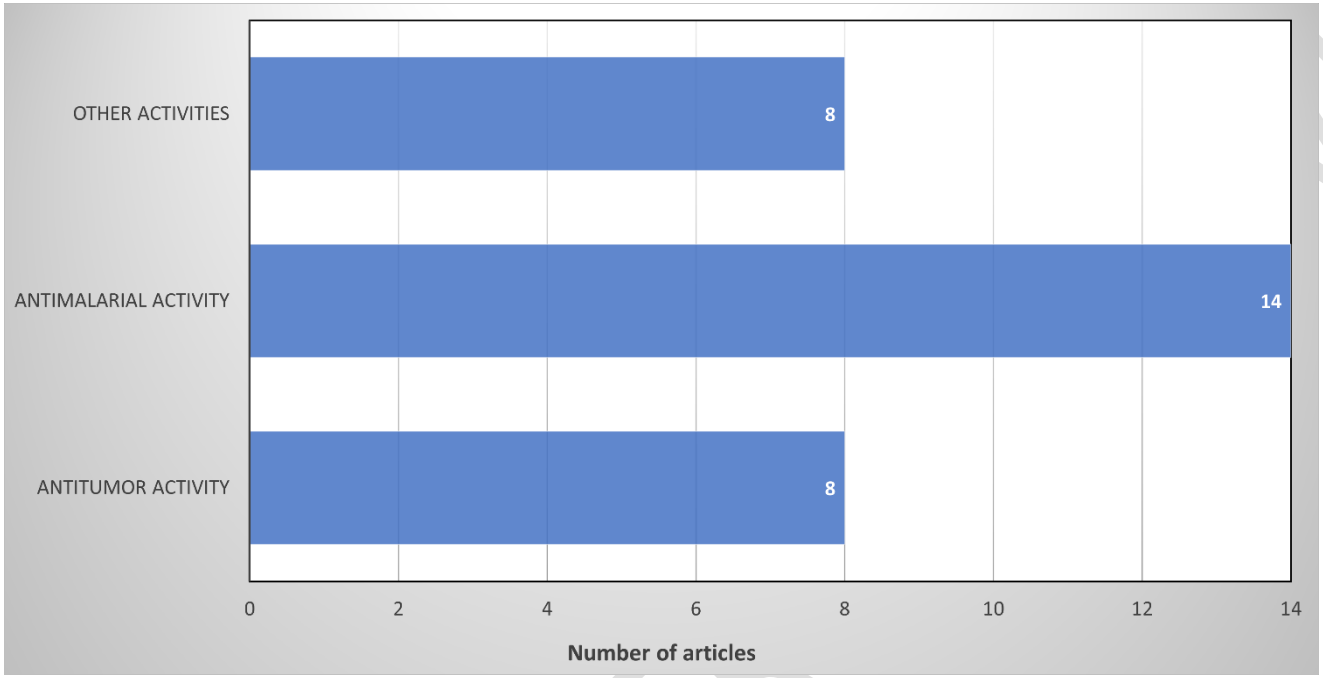

Source: the author.

Regarding the antitumor activity of NPs, it is observed that six out of the nine articles used the MTT assay (Ciapetti et al., 1993) – a tetrazolium-based calorimetric assay that analyzes cellular metabolic activity. The remaining two articles used the MTS assay, which is also based on a tetrazole compound and serves as a cell viability marker (Taddei et al., 2007), and the Trypan blue assay.

In one study by Zhou et al. (2017), they employed a fibroblast cell line (NIH3T3) and HeLa cells expressing GFP-LC3 (GFP-LC3/ HeLa). The cells exposed to photothermal NPs made of polidopamide and loaded with CQ diphosphate maintained a cell viability of approximately 80%. However, they showed greater photothermal sensitivity upon exposure to these NPs. In vitro pharmacokinetic tests demonstrated pH-dependent release, which increased in acidic mediums.

In the study by Feng et al. (2019), the MCF-7 breast adenocarcinoma cell line was used, and treatment with hollow NPs of mesoporous titanium dioxide loaded with HCQ sulfate resulted in a cell viability of 27.3 ± 1.8%. This demonstrated potentiation of sonodynamic therapy. In vitro pharmacokinetic tests showed a slow and sustained release of the drug.

Ma et al. (2018) also worked with the cervical cancer cell line HeLa and observed a cell viability of 33.20% after treatment with mesoporous NPs containing CQ. The treatment led to the inhibition of tumor-directed autophagy, resulting in increased cell death efficacy by photothermal therapy. In vitro pharmacokinetic assays demonstrated good and controllable thermo-induced release.

Shi et al. (2018) analyzed the effects on HeLa cells and HEK293 embryonic kidney cells. After treatment with metallic NPs containing CQ diphosphate, a viability of 49.4% and 75.8% was observed with the use of NPs FA-PEG/CQ@ZIF-8 and CQ@ZIF-8, respectively. The FA-PEG/CQ@ZIF-8 NPs increased CQ cytotoxicity and improved delivery to HeLa cells where RFs are overexpressed. In vitro pharmacokinetic tests demonstrated pH-dependent release (increased in an acidic medium).

Arya et al. (2018) conducted assays on basal epithelial cells of alveolar adenocarcinoma (A549) and cells derived from normal bronchial epithelium (BEAS-2B). Treatment with CQ-adsorbed graphene oxide nanoconjugate led to cell viability ranging from 80% to 45% in cancer cells. The nanoconjugate demonstrated excellent biocompatibility with normal cell lines. In vitro pharmacokinetic tests showed a pH-dependent release (about 31% of drug released in 72 h in a buffer solution).

Stagni et al. (2020) analyzed the effects of CQ-loaded trienylphosphonium cation-associated/functionalized polymer dendrimer on MCF-7, MDA-MB-231, and SK-BR-3 breast cancer cell lines. Cell viability was different for each strain, with viability being >25% (MCF-7); >50% (MDA-MB-231) and >55% (SK-BR-3). The carrier alone demonstrated some cytotoxicity against cancer cells, and the addition of CQ improved mitochondriotropic action, making it more selective to breast cancer strains.

Joshi et al. (2012) used the MCF-7 cell line and performed the intervention with gold NPs containing CQ. A cell viability below 80% was observed, indicating an increase in the cytotoxicity of GNP-CQ in relation to breast cancer cells.

The last article that analyzed antitumor activity was by Chen et al. (2019), which showed the lowest cell viability among the nine cited articles, ~20%. Murine mammary carcinoma cells (4T1) were used, and treatment with mesoporous NPs of silica incorporated in bismuth loaded with CQ was combined with photothermal treatment. The treatment led to reduced cell viability with increasing concentrations of NPs and prolonged irradiation time. In vitro pharmacokinetic tests demonstrated a controlled release by NIR light irradiation.

Table 2- Tumor Cytotoxicity

Reference	Cytotoxicity Assay _	Cell treated	Viability cell phone	Efficiency
Zhouet al. (2017)	MTT test	NIH3T3 and GFP-LC3/ HeLa cells	~ 80%,	These results revealed that the CQ autophagy inhibitor did indeed sensitize the photothermal death of cancer cells.
Fenget al. (2019)	MTT test	Lineage MCF-7 cell phone	27.3 ± 1.8%,	Implies that HCQ potentiated the effect of sonodynamic therapy
Maet al. (2018)	MTT test	HeLa cells	33.20%	(CQ + PCM) @HMPBs was able to induce inhibition of tumor-targeted autophagy to enhance cell killing efficacy by photothermal therapy.
Shiet al. (2018)	MTT test	HeLa cells or HEK293 cells	FA-PEG / CQ @ ZIF-8 and CQ @ ZIF-8 49.4 % and 75.8%, respectively	PEG/CQ @ ZIF-8 NPs increase CQ cytotoxicity and exhibit targeted delivery in HeLa cells where RFs are overexpressed.
Arya et al. (2018)	MTT test	A549 cells and BEAS-2B cells	ranged from 80% to 45 % (GO - Chl 1 to 100 ug /ml)	The results indicate excellent biocompatibility of the GO and GO- Chl nanoconjugates with normal cell lines.
Chenet al. (2019)	MTT test	4T1 cells	~20%	It was evident that cell viability was reduced with increasing concentrations of NPs and prolonged irradiation time.
Stagni et al. (2020)	MTS Assay	MCF-7, MDA-MB-231, SK-BR-3 cells	>25% (MCF-7); >50% (MDA-MB-231) and >55% (SK-BR-3)	PTTP-CQ had significantly higher cytotoxicity than PTPP alone, suggesting a mitochondriotropic action and greater selectivity to breast cancer cell lines.
Joshiet al. (2012)	Trypan blue assay	MCF-7 cells	<80%	An increased cytotoxicity of GNP - Chl against MCF-7 cells was observed.

CQ = Chloroquine; HCQ = hydroxichloroquine; NPs = Nanoparticles; NP = Nanoparticle

Table 3- Antimalarial Cytotoxicity

Reference	Cytotoxicity assay	Cell / strains treated	Viability cell phone	Toxicity hemolytic	Efficiency
Movellan et al. (2014)	Wst- 1 toxicity assay	HUVEC cells	It varies around 100-20% depending on the type and concentration of the polymer (log [polymer] = 1.5 to 4.0 ug /ml)	The respective IC50 values for drug-loaded C, D and dendron DB1 copolymers were 7, 204 and 466mg/ ml. Copolymer C demonstrated significant antimalarial activity in vitro at concentrations where cytotoxicity was not noted in HUVEC cells.	The respective IC50 values for drug-loaded C, D and dendron DB1 copolymers were 7, 204 and 466mg/ ml. Copolymer C demonstrated significant antimalarial activity in vitro at concentrations where cytotoxicity was not noted in HUVEC cells.
Kashyap et al. (2018)	Flow cytometry	Sensitive and resistant strains of *P. falciparum* (3D7 and RKL9)	IC50 of 0.031 µg /ml and 0.13 µg/ml, against strain 3D7 and RKL9, respectively.	Regarding biosafety, CHQ-DEX-NPs at 10, 100 and 1000-fold dilution exhibited 3.2%, 1.5% and 0.9% hemolysis.	1- The reduction in the inhibitory concentration of NPs can be attributed to the deposition of greater amounts of drug in food vacuoles of the parasites. 2- CHQ-DEX-NPs not induced hemolysis relevant in RBCs.
Medhi et al. (2018)	Susceptibility test	*P. falciparum* 3D7	The IC50 value for ihmpcl - CQDP was 25.14 nm	NI	The release of CQ from ihmPCL capsules proved to be very effective, with the drug being retained for a longer period of time and therefore a sustained delivery can suppress the growth of the *P.falciparum strain.*
Muga et al. (2018)	Hypoxanthine incorporation method	Sensitive and resistant strain of *P. falciparum (D6 and W2)*	IC50 4.752 ± 0.144 ng / ml and 2.41 ± 0.27 ng / ml for CQ-SLN and CQ- Hep -SLN, respectively.	NI	All SLNs exhibited increased antiplasmic activity compared to the standard CQ drug in the CQ-sensitive D6 strain, but no activity against the CQ-resistant W2 strain.
Fotoran et al. (2019)	Flow cytometry _	*P.bergheiNK65* - GFP strain	The IC50 with trapped QC is approximately four times lower than that for free QC added to the culture medium.	NI	Parasitemia was less than 40 % compared to treatment with twice the amount of the same drug administered without encapsulation.
Tripathy et al. (2018)	MTT test	Swiss mice infected with *P.berghei*	92% cell viability after isolation.	NI	Parasitemia decreased by 96.57% in the NCQ-treated group compared to the infected control group.
Tripathy et al. (2013)	Flow cytometry	Swiss mice infected with *P.*	NI	Cell death in the infected group was 18.16%, while in the group	Parasitemia in the NCQ-treated group was 00.73%.

		berghei NK65		treated with CQ it was 10.10% and, in the group, treated with NCQ it was 5.21%.	
Urbán et al. (2011)	FACS analysis	Cells infected with *P.falciparum*	26.7 ± 1.8% growth inhibition	NI	2 nM soluble CQ had virtually no effect on *P. falciparum* (3.4 ± 1.0% growth inhibition), whereas the same general concentration administered into targeted immunoliposomes induced 26.7 ± 1.8% inhibition of *P. falciparum*. growth of *P. falciparum*.
Baruahet al. (2018)	Peter's 4-day suppression test	C57BL/6 mice infected with 3D7 (sensitive) and RKL9 (resistant) strains of *P. falciparum*	IC_{50} of 12.8 ± 0.8 and 151.86 ± 10.88 ng /ml, respectively, against sensitive and resistant strains.	NI	1- The animals were completely cured, and the almost complete survival of the animals treated with the NLCs (survival rate of 83,33,66%). 2- NLCs loaded with CQ had better suppression of parasitemia and increased efficacy by over 23% compared to the pure drug.
Coma-Croset al. (2018)	Flow cytometry	Mice infected by *P. falciparum 3D7* and reinfected by *P.yoelii*	NI	NI	1- The group treated with the ISA23-CQ formulation had a survival of 60%. 2- When the nine surviving animals were reinfected with P. yoelii and left untreated, all recovered completely, without showing symptoms of the disease and with parasitemia levels below the microscopy detection limits.
Tripathy et al. (2014)	Flow cytometry	Swiss male mice infected with *P. berghei* NK65	The NCQ-treated group had a 97.59% decrease in parasitemia; also, the count of cell death markers had a decrease in liver (29.45%) and spleen (37.58%) compared to the group treated with free CQ.	NI	1- The NCQ-treated group demonstrated a 92.71% decrease in parasitaemia compared to the free CQ-treated group.
Urbán et al. (2011)	FACS analysis	RBC infected with *P. falciparum* strain 3D7	2 nm CQ or 360 nm phosmidomycin in solution decreased parasitosis by 3% or 6% when added to both the ring and trophozoid stages.	NI	Increasing the concentration of immunoliposomes containing 4 nM CQ results in a corresponding increase in the performance of the nanovector, reaching a 50% clear of parasitosis (for liposomes equipped with 250 antibody molecules).

Moles et al. (2015)	Microscopic counting of blood smears	immunodeficient mice (NOD scid gamma, NSG) grafted with human erythrocytes and infected IV. *with P. falciparum* 3D7	IC50 of about 35 nm	Erythrocyte viability was not compromised by iLP binding (immunoliposomes)	At a concentration of 50 nM of encapsulated CQ, parasite growth was completely inhibited. In comparison, free CQ was only able to completely inhibit the growth of *P. falciparum*when added to late-developing forms at a concentration of 200 nM.
Kudiratet al. (2019)	Microscopic examination of Wright's-stained thin blood smears	Albino mice infected with *Plasmodium berghei* NK65	NI	NI	Nanoencapsulation drastically reduced parasitemia and histopathological studies demonstrated liver tissue normalization.

NI = Not informed; CQ = Chloroquine; HCQ = hydroxichloroquine; NPs = Nanoparticles; NP = Nanoparticle

3.10. Cytotoxicity in Malaria Cells

Addressing the other fourteen articles that described the improvement of antimalarial activity, Table 3 shows different methods used for the evaluation, including flow cytometry, microscopic blood smear counting, FACS analysis, Peter's 4-day suppression test, MTT assay, hypoxanthine incorporation method, susceptibility assay, and WST-1 toxicity assay.

Movellan et al. (2014) tested CQ-loaded dendritic derivatives on human endothelial cells (HUVEC) using a WST-1 toxicity assay. The study demonstrated a cell viability range between 100% and 20% depending on the type and concentration of the polymer. The immunotoxicity of the copolymers and dendron DB1 was tested through hemolytic toxicity, showing IC50 values of 7, 204, and 466 mg/ml, respectively. Copolymer C demonstrated significant antimalarial activity in vitro at concentrations without cytotoxicity in HUVEC cells.

Kashyap et al. (2018) tested CQ-loaded polymeric NPs on sensitive and resistant strains of *P. falciparum* (3D7 and RKL9, respectively) using flow cytometry. The study obtained IC50 values of 0.031 µg/ml against 3D7 and 0.13 µg/ml against RKL9. The biosafety of CHQ-DEX-NPs exhibited low hemolysis at different dilutions.

Medhi et al. (2018) tested CQ diphosphate-loaded mesoporous NPs on red cells infected with *P. falciparum* 3D7. The susceptibility assay showed an IC50 value for ihmPCL-CQDP of 25.14 nM. No data were presented regarding hemolytic toxicity of normal cells.

Muga et al. (2018) tested the antimalarial cytotoxicity of heparin-functionalized solid lipid NPs (Hep-SLNs) loaded with CQ on sensitive and resistant strains of *P. falciparum* (D6 and W2). The study obtained IC50 values of 4.752 ± 0.144 mg/mL and 2.41 ± 0.27 mg/mL for CQ-SLN and CQ-Hep-SLN, respectively. The study demonstrated increased antiplasmodic activity of all SLNs compared to the standard CQ drug against the sensitive D6 strain but no activity against the CQ-resistant W2 strain.

Fotoran et al. (2019) analyzed the performance of multilamellar liposomes containing CQ in cells parasitized by the *P. berghei* strain NK65-GFP using flow cytometry. The study showed IC50 values of NPs with trapped QC approximately four times lower than those of free CQ administration.

Tripathy et al. (2018) analyzed the antimalarial cytotoxicity of polymeric NPs containing CQ in cells of Swiss mice infected with *P. berghei* using the MTT assay. The study demonstrated a decrease in parasitemia and reduction of apoptotic splenocytes.

Tripathy et al. (2013) analyzed the cytotoxicity of CQ-loaded polymeric NPs in cells from Swiss mice infected with *P. berghei* NK65 using flow cytometry. The study showed a significant reduction in parasitemia in the group treated with NPs compared to the other groups.

Baruah et al. (2018) tested CQ phosphate-loaded nanostructured lipid carriers in C7BL mice inoculated with sensitive (3D7) or resistant (RKL9) strains of *P. falciparum* using Peter's 4-day suppression test. The study demonstrated IC50 values of 12.8 ± 0.8 and 151.86 ± 10.88 mg/ml, respectively, against sensitive and resistant strains.

Coma-Cros et al. (2018) analyzed the antimalarial activity of CQ-loaded dendrimers in *P. falciparum* 3D7-infected and *P. yoelii*-reinfected mice using flow cytometry. The study showed that the group treated with the ISA23-CQ formulation had a survival rate of 60%.

Tripathy et al. (2014) analyzed the performance of dendrimers containing CQ in male Swiss mice infected with *P. berghei* NK65 using flow cytometry. The study demonstrated a decrease in parasitemia and a reduction of cell death markers.

Urbán et al. (2011b) tested immunoliposomes containing CQ or phosmidomycin on RBC infected with *P. falciparum* strain 3D7 through FACS analysis. The study showed a reduction in parasitosis with increasing concentrations of immunoliposomes containing CQ.

Kudirat et al. (2019) tested CQ phosphate release from metallic NPs in albino rats infected with *Plasmodium berghei* NK65 using microscopic examination of Wright-stained thin blood smears. The study demonstrated a sustained release and considerable reduction in parasitemia.

Finally, Moles et al. (2015) tested liposomes containing CQ or primaquine in female immunodeficient mice grafted with human erythrocytes and infected with *P. falciparum* 3D7. The study showed IC50 values for CQ at about 35nM, with complete inhibition of parasite growth at a concentration of 50nM. The study also showed no compromise in erythrocyte viability after the treatment. In vivo pharmacokinetic tests demonstrated a sustained release profile over 48 hours.

3.11. Other activities

The eight remaining articles tested various properties of nanoparticles (NPs) containing chloroquine (CQ) and/or hydroxychloroquine (HCQ):

Bhalekar et al. (2015) studied gel permeation of CQ-loaded solid lipid NPs on rat skin using an ex vivo test. The study demonstrated that the rate and extent of compound absorption were thermo-dependent, with passive drug diffusion. The gel nanoformulation showed greater retention on the skin compared to free CQ gel. In vivo tests on male Wistar rats showed that the nanogel formulation led to a greater reduction in paw volume than the standard treatment.

Liu et al. (2017) analyzed the relationship between inhibition and reduction in the rate of apoptosis caused by CQ-HCQ liposomes in lung fibroblasts isolated from bleomycin-treated rats. Alveolar macrophages were also isolated for treatment with CQ-HCQ, leading to a drastic reduction in inflammation induced by neutrophils in lung tissues. This confirmed the anti-fibrotic effect of the liposomes by inhibiting the growth factor CTGF. In vivo pharmacokinetic studies and safety assessment of liposomes and free HCQ sulfate in mice showed that the encapsulated form in CQ-HCQ liposomes provided a higher drug concentration in the blood for 24 hours due to sustained release, with reduced toxicity compared to free HCQ.

Usman; Akhyar Farrukh (2018) analyzed the release profile of CQ phosphate from iron polymeric NPs in vitro, showing a biphasic profile dependent on encapsulated CQ concentration, with a slow initial release and an accelerated secondary phase. The NPs also demonstrated bacterial inhibition capacity, inhibiting 26.31% to 47.36% of Staphylococcus culture. The study compared the hemolytic toxicity of the formulation with that of the free drug, showing that encapsulated CQ exhibited greater cytotoxicity over time.

Bhalekar et al. (2016) performed ex vivo assays of endocytic uptake of solid lipid NPs using an everted rat gut model. In vivo tests in male Wistar rats analyzed the pharmacokinetics and pharmacodynamics of the nanoformulation, observing paw volume and conducting histopathological assays. ELISA was used to evaluate the concentration of TNF-α at the site of inflammation. The results showed that encapsulation in a lipid matrix prevented hepatic degradation of the drug, leading to increased circulating Cmax. Bone erosion was reduced by 50% compared to the positive control group and 25% compared to the group treated with free CQ. ELISA demonstrated a considerable reduction in TNF-α secretion, indicating an interruption of disease progression.

Agrawal et al. (2007) tested the release of CQ by uncoated and galactose-coated poly-L-lysine dendrimers in vitro. The study showed a slower and more sustained release profile and low hemolytic toxicity, particularly in the coated NPs. In vivo tests were performed to determine the blood level of the drug and to count red blood cells, leukocytes, and lymphocytes. The results demonstrated that the initial concentration of the encapsulated drug was lower than that of the free drug but remained in circulation for a longer time. Ex vivo studies of NP uptake by macrophages showed that coating with galactose reduced the uptake rate.

Lima et al. (2018) analyzed the activity of polymeric NPs containing CQ diphosphate in Vero cells in vitro. Cell viability assays were conducted at different concentrations of CQ, CQ-NP, and white NPs (B-NP) incubated between 24 and 48 hours. The study observed that cytotoxicity was dependent on the drug concentration, with the IC50 value three times lower for the nanoformulation than for the free drug. This characteristic was related to the greater uptake of the nanoencapsulated drug. Antiviral activity against HSV-1 was evaluated using the standard plaque reduction assay in Vero E6 cells infected with HSV-1, showing total inhibition of viral replication with 30 µg/mL of free CQ and only 10 µg/mL of the nanoformulation.

Crommelin et al. (1991) tested the activity of CQ-containing liposomes in vivo by subcutaneous and intramuscular injections in Swiss mice. Subcutaneous administration of doses of the fluid or gel nanoformulation provided ten days of protection against potentially lethal *Plasmodium berghei* infection, whereas the administration of the maximum dose (0.8 mg/mouse) of free CQ did not confer resistance to the group. The encapsulated form of the drug did not induce toxic release peaks or hepatic/splenic accumulation.

Bhadra & Jain (2006) tested the hemolytic toxicity of CQ-loaded peptide dendrimers in vitro on cell lines PL15K4G, PL15K5G, PL4K4G, and PL4K5G. The study showed low hemolytic toxicity, mainly when coated with sulfate of chondroitin A (CSA). Studies were also carried out on the interaction of dendrimers with macrophages and on the cytoadherence of CSA-coated NPs. The blood level and biodistribution of CQ were analyzed based on the formulation and route of administration, showing that coating with CSA reduced the rate of phagocytosis. No hemolytic toxicity was observed in normal cells, and encapsulation and coating gave the drug a sustained release profile, increased bioavailability, and reduced side effects due to greater specificity in the drug's performance.

4. Conclusion

It can be asserted that the nanoencapsulation of the drugs CQ and/or HCQ led to an increase in specificity, as the side effects caused by the toxic accumulation of the drug were mitigated. It also extended the drug release time, enabling a longer treatment duration with the same drug concentration without inducing toxic peaks. An increase in effectiveness was also demonstrated in malarial cells resistant to CQ, given the greater cytotoxicity in parasitized cells. There was also the sensitization of cancer cells, a characteristic with high clinical potential for chemotherapies, sonodynamic therapy, and photothermal therapy. The nanoencapsulation reduced drug loss by hepatic clearance and also decreased drug uptake by phagocytes, especially when NPs were coated with biocompatible compounds such as PEG.

Therefore, the nanometric formulation proved to be extremely advantageous for the drugs addressed and provided a range of possible clinical applications. Many other effects were tested, and the application opportunities proved to be innovative and advantageous, which can be explored in the near future.

REFERENCES

Agrawal, P., Gupta, U., & Jain, N. K. (2007). Glycoconjugated peptide dendrimers-based nanoparticulate system for the delivery of chloroquine phosphate. Biomaterials, 28(22), 3349–3359.

Alex, A., Paul, W., Chacko, A. J., & Sharma, C. P. (2011). Enhanced delivery of lopinavir to the CNS using Compritol®-based solid lipid nanoparticles. Therapeutic Delivery, 2(1), 25–35.

Amoabediny, G., Haghiralsadat, F., Naderinezhad, S., et al. (2018). Overview of preparation methods of polymeric and lipid-based (niosome, solid lipid, liposome) nanoparticles: A comprehensive review. International Journal of Polymeric Materials and Polymeric Biomaterials, 67(6), 383–400.

Arya, B. D., Mittal, S., Joshi, P., et al. (2018). Graphene oxide-chloroquine nanoconjugate induce necroptotic death in A549 cancer cells through autophagy modulation. Nanomedicine (Lond), 13(18), 2261–2282.

Bangun, H., Tandiono, S., & Arianto, A. (2018). Preparation and evaluation of chitosan-tripolyphosphate nanoparticles suspension as an antibacterial agent. Journal of Applied Pharmaceutical Science, 8(12), 147–156.

Baruah, U. K., Gowthamarajan, K., Ravisankar, V., et al. (2018). Optimisation of chloroquine phosphate loaded nanostructured lipid carriers using Box–Behnken design and its antimalarial efficacy. J Drug Target, 26(7), 576–591.

Bhadra, D., Bhadra, S., & Jain, N. K. (2006). PEGylated peptide dendrimeric carriers for the delivery of antimalarial drug chloroquine phosphate. Pharm Res, 23(3), 623–633.

Bhadra, D., Bhadra, S., & Jain, N. K. (2005). Pegylated lysine based copolymeric dendritic micelles for solubilization and delivery of artemether. Journal of Pharmacy and Pharmaceutical Sciences, 8(3), 467–482.

Bhalekar, U., & Madgulkar, A. R. (2016). Fabrication and efficacy evaluation of chloroquine nanoparticles in CFA-induced arthritic rats using TNF-alpha ELISA. European Journal of Pharmaceutical Sciences, 84, 1–8.

Bhalekar, M. R., Upadhaya, P. G., Nalawade, S. D., Madgulkar, A. R., & Kshirsagar, S. J. (2015). Anti-rheumatic activity of chloroquine-SLN gel on Wistar rats using complete Freund's adjuvant (CFA) model. Indian Journal of Rheumatology, 10(2), 58–64.

Chen, T., Cen, D., Ren, Z. H., et al. (2019). Bismuth embedded silica nanoparticles loaded with autophagy suppressant to promote photothermal therapy. Biomaterials, 221, 9.

Ciapetti, G., Cenni, E., Pratelli, L., & Pizzoferrato, A. (1993). In vitro evaluation of cell/biomaterial interaction by MTT assay. Biomaterials, 14(5), 359–364.

Coma-Cros, E. M., Biosca, A., Marques, J., et al. (2018). Polyamidoamine nanoparticles for the oral administration of antimalarial drugs. Pharmaceutics, 10(4).

Crommelin, D. J. A., Eling, W. M. C., Steerenberg, P. A., et al. (1991). Liposomes and immunoliposomes for controlled release or site-specific delivery of anti-parasitic drugs and cytostatics. Journal of Controlled Release, 16(1), 147–154.

Desai, P. P., Date, A. A., Patravale, V. B. (2011). Overcoming poor oral bioavailability using nanoparticle formulations - Opportunities and limitations. Drug Discovery Today: Technologies, 9(2), 87-95.

Doostmohammadi, A., Monshi, A., Salehi, R., Mohammad Hossein Fathi, Zahra Golniya, & Daniels, A. U. (2011). Bioactive glass nanoparticles with negative zeta potential. Ceramics International, 37(7), 2311–2316. https://doi.org/10.1016/j.ceramint.2011.03.026

Ealias, A. M., & Saravanakumar, M. P. (2017). A review on the classification, characterisation, synthesis of nanoparticles and their application. IOP Conference Series: Materials Science and Engineering, 263(3).

Eloy, J. O., Petrilli, R., Trevizan, L. N. F., & Chorilli, M. (2017). Immunoliposomes: A review on functionalization strategies and targets for drug delivery. Colloids and Surfaces B: Biointerfaces, 159, 454–467.

Feng, Q. H., Yang, X. M., Hao, Y. T., et al. (2019). Cancer cell membrane-biomimetic nanoplatform for enhanced sonodynamic therapy on breast cancer via autophagy regulation strategy. ACS Appl Mater Interfaces, 11(36), 32729–32738.

Fotoran, W. L., Münteferring, T., Kleiber, N., et al. (2019). A multilamellar nanoliposome stabilized by interlayer hydrogen bonds increases antimalarial drug efficacy. Nanomedicine, 22, 102099.

Grasso, G., Colella, F., Forciniti, S., Onesto, V., Iuele, H., Siciliano, A., Carnevali, F., Chandra, A., Gigli, G., & Loretta. (2023). Fluorescent nano- and microparticles for sensing cellular microenvironment: past, present and future applications. Nanoscale Advances, 5(17), 4311–4336. https://doi.org/10.1039/d3na00218g

Honary, S., & Zahir, F. (2013). Effect of Zeta Potential on the Properties of Nano-Drug Delivery Systems - A Review (Part 1). Tropical Journal of Pharmaceutical Research, 12(2), 255–264. [Faculty of Pharmacy, University of Benin]

Jain, A., Kesharwani, P., Garg, N. K., et al. (2015). Galactose engineered solid lipid nanoparticles for targeted delivery of doxorubicin. Colloids and Surfaces B: Biointerfaces, 134, 47–58.

Joglekar, M., & Trewyn, B. G. (2013). Polymer-based stimuli-responsive nanosystems for biomedical applications. Biotechnology Journal, 8(8), 931–945. https://doi.org/10.1002/biot.201300073

Johnston, S. T., Faria, M., & Crampin, E. J. (2018). An analytical approach for quantifying the influence of nanoparticle polydispersity on cellular delivered dose. Journal of the Royal Society Interface, 15(144).

Joshi, P., Chakraborti, S., Ramirez-Vick, J. E., et al. (2012). The anticancer activity of chloroquine-gold nanoparticles against MCF-7 breast cancer cells. Colloids Surf B Biointerfaces, 95, 195–200.

K. Jayamoorthy, Rajagopalan, N. R., Prakash, S. M., B. Subash, G. Murugan, K.I. Dhanalekshmi, Suresh, S., R. Sasikala, K. Saravanan, & M. Venkatesh Perumal. (2023). Catalytic synthesis and characterization of aryl benzimidazole and its interaction with TiO2 nanoparticles: ESIPT process. Chemical Physics Impact, 6, 100184–100184. https://doi.org/10.1016/j.chphi.2023.100184

Kankala, R. K., Zhang, H., Liu, C. G., et al. (2019). Metal Species–Encapsulated Mesoporous Silica Nanoparticles: Current Advancements and Latest Breakthroughs. Advanced Functional Materials, 29(43), 1–42.

Kashyap, A., Kaur, R., Baldi, A., et al. (2018). Chloroquine diphosphate bearing dextran nanoparticles augmented drug delivery and overwhelmed drug resistance in Plasmodium falciparum parasites. Int J Biol Macromol, 114, 161–168.

Kudirat, S. O., Tawakalitu, A., Saka, A. A., et al. (2019). Entrapped chemically synthesized gold nanoparticles combined with polyethylene glycol and chloroquine diphosphate as an improved antimalarial drug. Nanomedicine Journal, 6(2), 85–96.

Lima, T. L. C., Feitosa, R. D., Dos Santos-Silva, E., et al. (2018). Improving Encapsulation of Hydrophilic Chloroquine Diphosphate into Biodegradable Nanoparticles: A Promising Approach against Herpes Virus Simplex-1 Infection. Pharmaceutics, 10(4), 18.

Liu, L., Ren, J., He, Z., Men, K., Mao, Y., Ye, T., Chen, H., Li, L., Xu, B., Wei, Y., & Wei, X. (2017). Cholesterol-modified hydroxychloroquine-loaded nanocarriers in bleomycin-induced pulmonary fibrosis. Scientific Reports, 7, 10737. https://doi.org/10.1038/s41598-017-11450-3

Lowry, G., Hill, R. J., Harper, S., Rawle, A. F., Hendren, C. O., Klaessig, F., Nobbmann, U., Sayre, P., & Rumble, J. (2016). Guidance to improve the scientific value of zeta-potential measurements in nanoEHS. Environmental Science: Nano, 3, 953–965. https://doi.org/10.1039/c6en00136j

Lu, Y., Aimetti, A. A., Langer, R., & Gu, Z. (2016). Bioresponsive materials. Nature Reviews Materials, 2(1). https://doi.org/10.1038/natrevmats.2016.75

Luo, R., Zhang, J., Zhuang, W., Deng, L., Li, L., Yu, H., Wang, J., Huang, N., & Wang, Y. (2018). Multifunctional coatings that mimic the endothelium: Surface-bound active heparin nanoparticles with in situ generation of nitric oxide from nitrosothiols. Journal of Materials Chemistry B, 6, 5582. https://doi.org/10.1039/c8tb00596f

Ma, Y., Chen, H. J., Hao, B. M., Zhou, J. H., He, G., Miao, Z. H., Xu, Y., Gao, L., Zhou, W., & Zha, Z. B. (2018). A chloroquine-loaded Prussian blue platform with controllable autophagy inhibition for enhanced photothermal therapy. Journal of Materials Chemistry B, 6(7). https://doi.org/10.1039/c8tb01987h

Manmode, A. S., Sakarkar, D. M., & Mahajan, N. M. (2009). Nanoparticles-tremendous therapeutic potential: A review. International Journal of PharmTech Research, 1, 1020–1027.

Manzano, M., & Vallet-Regí, M. (2020). Mesoporous silica nanoparticles for drug delivery. Advanced Functional Materials, 30, 3–5. https://doi.org/10.1002/adfm.201902634

Marques, J., Valle-Delgado, J. J., Urbán, P., Baró, E., Prohens, R., Mayor, A., Cisteró, P., Delves, M., Sinden, R. E., Grandfils, C., de Paz, J. L., García-Salcedo, J. A., & Fernàndez-Busquets, X. (2017). Adaptation of targeted nanocarriers to changing requirements in antimalarial drug delivery. Nanomedicine: Nanotechnology, Biology, and Medicine, 13, 515–525. https://doi.org/10.1016/j.nano.2016.09.010

Medhi, H., Maity, S., Suthram, N., Chalapareddy, S. K., Bhattacharyya, M. K., & Paik, P. (2018). Hollow mesoporous polymer capsules with Dihydroartemisinin and Chloroquine diphosphate for knocking down Plasmodium falciparum infection. Biomedical Physics & Engineering Express, 4. https://doi.org/10.1088/2057-

1976/aaaddb

M.M. Salem-Bekhit, M. Da'i, M.M. Rakhmatullaeva, M. Mirzaei, S. Al Zahrani, & N.A. Alhabib. (2023). The drug delivery of methimazole through the sensing function assessments of BeO fullerene-like particles: DFT study. Chemical Physics Impact, 7, 100335–100335. https://doi.org/10.1016/j.chphi.2023.100335

Mody, V., Siwale, R., Singh, A., & Mody, H. (2010). Introduction to metallic nanoparticles. Journal of Pharmaceutics & Bioallied Sciences, 2, 282. https://doi.org/10.4103/0975-7406.72127

Mohanraj, V. J., & Chen, Y. (2007). Nanoparticles - A review. Tropical Journal of Pharmaceutical Research, 5, 561–573.https://doi.org/10.4314/tjpr.v5i1.14634

Moles, E., Urbán, P., Jiménez-Díaz, M. B., Viera-Morilla, S., Angulo-Barturen, I., Busquets, M. A., & Fernàndez-Busquets, X. (2015). Immunoliposome-mediated drug delivery to Plasmodium-infected and non-infected red blood cells as a dual therapeutic/prophylactic antimalarial strategy. Journal of Controlled Release, 210, 217–229. https://doi.org/10.1016/j.jconrel.2015.05.284

Movellan, J., Urbán, P., Moles, E., de la Fuente, J. M., Sierra, T., Serrano, J. L., & Fernàndez-Busquets, X. (2014). Amphiphilic dendritic derivatives as nanocarriers for the targeted delivery of antimalarial drugs. Biomaterials, 35, 7940–7950. https://doi.org/10.1016/j.biomaterials.2014.05.061

Muga, J. O., Gathirwa, J. W., Tukulula, M., & Jura, W. G. Z. O. (2018). In vitro evaluation of chloroquine-loaded and heparin surface-functionalized solid lipid nanoparticles. Malaria Journal, 17. https://doi.org/10.1186/s12936-018-2302-9

Ngoepe, M., Choonara, Y. E., Tyagi, C., Tomar, L. K., du Toit, L. C., Kumar, P., Ndesendo, V. M. K., & Pillay, V. (2013). Integration of Biosensors and Drug Delivery Technologies for Early Detection and Chronic Management of Illness. Sensors (Basel, Switzerland), 13(6), 7680–7713. https://doi.org/10.3390/s130607680

Nie, W., Zhang, B., Pan, R., Wang, S., Yan, X., Tan, J. (2019). Surface modification with chondroitin sulfate targets nanoparticles to the neuronal cell membrane in the substantia nigra. ACS Chemical Neuroscience, 10(11), 4994-5003. https://doi.org/10.1021/acschemneuro.9b00597

Nie, Y., Li, J., Ding, H., Xie, L., Li, L., He, B., Wu, Y., & Gu, Z. (2012). Cholesterol derivatives based charged liposomes for doxorubicin delivery: Preparation, in vitro and in vivo characterization. Theranostics, 2(11), 1092–1103. https://doi.org/10.7150/thno.4949

Nikam, A. P., Ratnaparkhi, M. P., & Chaudhari, S. P. (2014). Review Article NANOPARTICLES – AN OVERVIEW. Indian Journal of Pharmacy and Pharmacology, 3, 1121–1127.

Odiongenyi, A. O. (2019). Removal of Ethyl Violet Dye from Aqueous Solution by Graphite Dust and Nano Graphene Oxide Synthesized from Graphite Dust, 4, 103–109.

Pelt, J., Busatto, S., Ferrari, M., Thompson, E. A., Mody, K., & Wolfram, J. (2018). Chloroquine and nanoparticle drug delivery: A promising combination. Pharmacology & Therapeutics, 191, 43–49. https://doi.org/10.1016/j.pharmthera.2018.06.007

Poinard, B., Zhan, S., Neo, Y., Li, E., Yeo, L., Peng, H., Gee Neoh, K., Chen, J., & Kah, Y. (2018). Polydopamine nanoparticles enhance drug release for combined photodynamic and photothermal therapy. ACS Applied Materials & Interfaces, 10(33), 27466-27473. https://doi.org/10.1021/acsami.8b04799

Saravanan, P., Jayamoorthy, K., & Anandakumar, S. (2016). Fluorescence quenching of APTES by Fe2O3 nanoparticles – Sensor and antibacterial applications. Journal of Luminescence, 178, 241–248. https://doi.org/10.1016/j.jlumin.2016.05.031

Schrezenmeier, E. &Dörner, T. (2020). Mechanisms of action of hydroxychloroquine and chloroquine: implications for rheumatology. Nature Reviews Rheumatology, 16(3), 155-166.

Shazly, G. A. (2017). Corrigendum to "Ciprofloxacin Controlled-Solid Lipid Nanoparticles: Characterization, In Vitro Release, and Antibacterial Activity Assessment". BioMed Research International, 2017, 6761452. https://doi.org/10.1155/2017/6761452

Shazly, G. A. (2017). Corrigendum to "Ciprofloxacin Controlled-Solid Lipid Nanoparticles: Characterization, In Vitro

Release, and Antibacterial Activity Assessment". BioMed Research International, 2017, 6761452. https://doi.org/10.1155/2017/6761452

Shi, Z. Q., Chen, X. R., Zhang, L., Ding, S. P., Wang, X., Lei, Q. F., Fang, W. J. (2018). FA-PEG decorated MOF nanoparticles as a targeted drug delivery system for controlled release of an autophagy inhibitor. Biomaterials Science, 6(10), 2754–2762. https://doi.org/10.1039/c8bm00625c

Stagni, V., Kaminari, A., Sideratou, Z., Sakellis nvestigation, E., Vlahopoulos, S. A., & Tsiourvas, D. (2020). Targeting breast cancer stem-like cells using Chloroquine encapsulated by a Triphenylphosphonium-functionalized hyperbranched polymer. International Journal of Pharmaceutics, 119465. https://doi.org/https://doi.org/10.1016/j.ijpharm.2020.119465

Stevens, D. M., Crist, R. M., & Stern, S. T. (2020). Reformulation of Chloroquine and Hydroxychloroquine. Molecules, 26(1), 175. https://doi.org/10.3390/molecules26010175

Suresh, S., Jayamoorthy, K., & Karthikeyan, S. (2016). Fluorescence sensing of potential NLO material by bunsenite NiO nanoflakes: Room temperature magnetic studies. Sensors and Actuators B: Chemical, 232, 269–275. https://doi.org/10.1016/j.snb.2016.03.1490POPO

Suresh, S., K. Jayamoorthy, & Karthikeyan, S. (2018). Switch-on fluorescence of 5-amino-2-mercapto benzimidazole by Mn3O4 nanoparticles: Experimental and theoretical approach. Journal of Luminescence, 198, 28–33. https://doi.org/10.1016/j.jlumin.2018.02.005

Taddei, E. B., Bueno, T., Henriques, V. A. R., Silva, C. R. M., Cairo, C. A. A., & Bottino, M. C. (2007). Ensaio de Citotoxicidade e Influência do Tratamento de Solubilização na Microestrutura da Liga Ti-35Nb-7Zr-5Ta para Potenciais Aplicações Ortopédicas. Revista Matéria, 12, 120–127.

Tomaszewska, E., Soliwoda, K., Kadziola, K., Tkacz-Szczesna, B., Celichowski, G., Cichomski, M., Szmaja, W., Grobelny, J. (2013). Detection limits of DLS and UV-Vis spectroscopy in characterization of polydisperse nanoparticles colloids. Journal of Nanomaterials, 2013. https://doi.org/10.1155/2013/313081

Tomitaka, A., Arami, H., Huang, Z., Raymond, A., Rodriguez, E., Cai, Y., Febo, M., Takemura, Y., & Nair, M. (2018). Hybrid magneto-plasmonic liposomes for multimodal image-guided and brain-targeted HIV treatment. Nanoscale, 10(1), 184–194. https://doi.org/10.1039/c7nr07255d

Tripathy, S., Chattopadhyay, S., Dash, S. K., Matsabisa, M. G., & Roy, S. (2018). Nano chloroquine delivery against Plasmodium berghei NK65 induced programmed cell death in spleen. Asian Pacific Journal of Tropical Medicine, 11(9), 540–546. https://doi.org/10.4103/1995-7645.242312

Tripathy, S., Das, S., Dash, S. K., Mahapatra, S. K., Chattopadhyay, S., Majumdar, S., Pramanik, P., Roy, S. (2014). A prospective strategy to restore the tissue damage in malaria infection: Approach with chitosan-trypolyphosphate conjugated nanochloroquine in Swiss mice. European Journal of Pharmacology, 737, 11–21. https://doi.org/10.1016/j.ejphar.2014.04.030

Tripathy, S., Mahapatra, S. K., Chattopadhyay, S., Das, S., Dash, S. K., Majumder, S., Pramanik, P., Roy, S. (2013). A novel chitosan based antimalarial drug delivery against Plasmodium berghei infection. Acta Tropica, 128(3), 494–503. https://doi.org/10.1016/j.actatropica.2013.07.011

Urbán, P., Estelrich, J., Adeva, A., Cortés, A., & Fernàndez-Busquets, X. (2011). Study of the efficacy of antimalarial drugs delivered inside targeted immunoliposomal nanovectors. Nanoscale Research Letters, 6, 620. https://doi.org/10.1186/1556-276X-6-620

Urbán, P., Estelrich, J., Cortés, A., & Fernàndez-Busquets, X. (2011). A nanovector with complete discrimination for targeted delivery to Plasmodium falciparum-infected versus non-infected red blood cells in vitro. Journal of Controlled Release, 151(3), 202–211. https://doi.org/10.1016/j.jconrel.2011.01.001

Usman, M., & Akhyar Farrukh, M. (2018). Delayed release profile of iron nano-chloroquine phosphate and evaluation of its toxicity. Materials Today Proceedings, 5(19), 15645–15652. https://doi.org/https://doi.org/10.1016/j.matpr.2018.04.174

Van Vlerken, L. E., Vyas, T. K., & Amiji, M. M. (2007). Poly(ethylene glycol)-modified nanocarriers for tumor-targeted and intracellular delivery. Expert Review of Medical Devices, 4(4), 463–478. https://doi.org/10.1586/17434440.4.4.463

Wang, L., Shen, C., & Cao, Y. (2019). PVP modified Fe3O4@SiO2 nanoparticles as a new adsorbent for hydrophobic substances. Journal of Physics and Chemistry of Solids, 130, 56–60. https://doi.org/10.1016/j.jpcs.2019.05.004

Yee Fam, S., Fei Chee, C., Yeah Yong, C., Lian Ho, K., Razak Mariatulqabtiah, A., Siang Tan, W. (n.d.). Stealth Coating of Nanoparticles in Drug-Delivery Systems. https://doi.org/10.3390/nano10040787

Yoo, M. K., Park, I. K., Lim, H. T., Lee, S. J., Jiang, H. L., Kim, Y. K., Choi, Y. J., Cho, M. H., & Cho, C. S. (2012). Folate-PEG-superparamagnetic iron oxide nanoparticles for lung cancer imaging. Acta Biomaterialia, 8(8), 3005–3013. https://doi.org/10.1016/j.actbio.2012.04.029

Youssef, K., Ullah, A., Rezai, P., Hasan, A., & Alidad Amirfazli. (2023). Recent advances in biosensors for real time monitoring of pH, temperature, and oxygen in chronic wounds. Materials Today Bio, 22, 100764–100764. https://doi.org/10.1016/j.mtbio.2023.100764

Zhang, Y., Yang, M., Portney, N. G., Cui, D., Budak, G., Ozbay, E., Ozkan, M. (2007). Zeta potential: A surface electrical characteristic to probe the interaction of nanoparticles with normal and cancer human breast epithelial cells. Biomedical Microdevices, 9(6), 787–796. https://doi.org/10.1007/s10544-007-9139-2

Zhou, Z. J., Yan, Y., Hu, K. W., Zou, Y., Li, Y. W., Ma, R., Zhang, Q., & Cheng, Y. Y. (2017). Autophagy inhibition enabled efficient photothermal therapy at a mild temperature. Biomaterials, 141, 116–124. https://doi.org/10.1016/j.biomaterials.2017.06.030

Zhu, Z., & Su, M. (2017). Polydopamine nanoparticles for combined chemo-and photothermal cancer therapy. ACS Applied Materials & Interfaces, 7(25), 16883-16891. https://doi.org/10.1021/acsami.5b03194
oi.org/10.1021/acsami.5b03194